Synthesis and Structural Characterization of Helix-Forming β-Peptides: *trans*-2-Aminocyclopentanecarboxylic Acid Oligomers

Daniel H. Appella, Laurie A. Christianson, Daniel A. Klein, Michele R. Richards, Douglas R. Powell, and Samuel H. Gellman*

Contribution from the Department of Chemistry, University of Wisconsin, Madison, Wisconsin 53706-1396

Received April 14, 1999

Abstract: Synthetic protocols and circular dichroism (CD) spectra are reported for a series of oligomers of (*R,R*)-*trans*-2-aminocyclopentanecarboxylic acid (*trans*-ACPC). The two longest oligomers, a hexamer and an octamer, have also been examined crystallographically. Both crystal structures show that the β-peptide backbone adopts a regular helix that is defined by a series of interwoven 12-membered ring hydrogen bonds ("12-helix"). Each hydrogen bond links a carbonyl oxygen to an amide proton three residues toward the C-terminus. CD data suggest that the conformational preference of *trans*-ACPC oligomers in methanol is strongly length-dependent, which implies that 12-helix formation is a cooperative process, as seen for the α-helix formed by conventional peptides. Previous work has established that oligomers and polymers of β-amino acids can adopt helical conformations, but the 12-helix is an unprecedented β-peptide secondary structure.

Unnatural oligomers that adopt well-defined conformations, similar to those displayed by proteins and RNA, are a subject of increasing interest to chemists.[1−18] We use the term "foldamers" to describe this subset of oligomers, because most oligomers do not have strong conformational preferences. Creation of new foldamers tests and refines our ability to understand how networks of noncovalent interactions promote adoption of specific shapes by flexible molecules. In addition to this fundamental motivation, foldamer research has practical significance because oligomers with predictable conformations should provide new strategies for mimicry of biomolecular function. For example, foldamers that adopt robust helical or sheet secondary structures may allow one to mimic helices or sheets displayed on the surfaces of folded proteins. A foldamer that mimics a helix or sheet involved in a protein−protein recognition site could inhibit the recognition process.[19] Alter-

* To whom correspondence should be addressed.

(1) Review: Gellman, S. H. *Acc. Chem. Res.* **1998**, *31*, 173.

(2) β-Peptide folding: (a) Seebach, D.; Overhand, M.; Kühnle, F. N. M.; Martinoni, B.; Oberer, L.; Hommel, U.; Widmer, H. *Helv. Chim. Acta* **1996**, *79*, 913. (b) Seebach, D.; Ciceri, P.; Overhand, M.; Juan, B.; Rigo, D.; Oberer, L.; Hommel, U.; Amstutz, R.; Widmer, H. *Helv. Chim. Acta* **1996**, *79*, 2043. (c) Seebach, D.; Matthews, J. L. *J. Chem. Soc., Chem. Commun.* **1997**, 2015−2022. (d) Seebach, D.; Abele, S.; Gademann, K.; Guichard, G.; Hintermann, T.; Jaun, B.; Matthews, J. L.; Schreiber, J.; Oberer, L.; Hommel, U.; Widmer, H. *Helv. Chim. Acta* **1998**, *81*, 932. (e) Seebach, D.; Abele, S.; Sifferlen, T.; Hänggi, M.; Gruner, S.; Seiler, P. *Helv. Chim. Acta* **1998**, *81*, 2218.

(3) β-Peptide folding: (a) Appella, D. H.; Christianson, L. A.; Karle, I. L.; Powell, D. R.; Gellman, S. H. *J. Am. Chem. Soc.* **1996**, *118*, 13071. (b) Appella, D. H.; Christianson, L. A.; Klein, D. A.; Powell, D. R.; Huang, X.; Barchi, J. J.; Gellman, S. H. *Nature* **1997**, *387*, 381. (c) Krauthäuser, S.; Christianson, L. A.; Powell, D. R.; Gellman, S. H. *J. Am. Chem. Soc.* **1997**, *119*, 11719. (d) Chung, Y. J.; Christianson, L. A.; Stanger, H. E.; Powell, D. R.; Gellman, S. H. *J. Am. Chem. Soc.* **1998**, *120*, 10555. (e) Appella, D. H.; Barchi, J. J.; Durell, S.; Gellman, S. H. *J. Am. Chem. Soc.* **1999**, *121*, 2309. (f) Appella, D. H.; Christianson, L. A.; Karle, I. L.; Powell, D. R.; Gellman, S. H. *J. Am. Chem. Soc.* **1999**, *121*, 6206.

(4) β-Peptide folding: (a) Diederichsen, U.; Schmitt, H. W. *Eur. J. Org. Chem.* **1998**, 827. (b) Gung, B. W.; Zou, D.; Stalcup, A. M.; Cottrell, C. E. *J. Org. Chem.* **1999**, *64*, 2176.

(5) Vinylogous peptide folding: Hagihara, M.; Anthony, N. J.; Stout, T. J.; Clardy, J.; Schreiber, S. L. *J. Am. Chem. Soc.* **1992**, *114*, 6568.

(6) Nucleic acid analogue folding: Beier, M.; Reck, F.; Wagner, T.; Krishnamurthy, R.; Eschenmoser, A. *Science* **1999**, *283*, 699 and references therein.

(7) Aedamer folding: (a) Lokey, R. S.; Iverson, B. L. *Nature* **1995**, *375*, 303. (b) Nguyen, J. Q.; Iverson, B. L. *J. Am. Chem. Soc.* **1999**, *121*, 2639.

(8) Sulfonamide oligomer folding: Gennari, C.; Salom, B.; Potenza, D.; Longari, C.; Fioravanzo, E.; Carugo, O.; Sardone, N. *Chem. Eur. J.* **1996**, *2*, 644 and references therein.

(9) γ-Peptide folding: (a) Hintermann, T.; Gademann, K.; Jaun, B.; Seebach, D. *Helv. Chim. Acta* **1998**, *81*, 983. (b) Hanessian, S.; Luo, X.; Schaum, R.; Michnick, S. *J. Am. Chem. Soc.* **1998**, *120*, 8569.

(10) δ-Peptide folding: (a) Szabo, L.; Smith, B. L.; McReynolds, K. D.; Parrill, A. L.; Morris, E. R.; Gervay, J. *J. Org. Chem.* **1998**, *63*, 1074. (b) Smith, M. D.; Claridge, T. D. W.; Tranter, G. E.; Sansom, M. S. P.; Fleet, G. W. J. *J. Chem. Soc., Chem. Commun.* **1998**, 2041. (c) Long, D. D.; Hungerford, N. L.; Smith, M. D.; Brittain, D. E. A.; Marquess, D. G.; Claridge, T. D. W.; Fleet, G. W. J. *Tetrahedron Lett.* **1999**, *40*, 2195. (d) Claridge, T. D. W.; Long, D. D.; Hungerford, N. L.; Aplin, R. T.; Smith, M. D.; Marquess, D. G.; Fleet, G. W. J. *Tetrahedron Lett.* **1999**, *40*, 2199.

(11) Oligourea folding: Nowick, J. S.; Mahrus, S.; Smith, E. M.; Ziller, J. W. *J. Am. Chem. Soc.* **1996**, *118*, 1066.

(12) Anthranilic acid oligomer folding: Hamuro, Y.; Geib, S. J.; Hamilton, A. D. *J. Am. Chem. Soc.* **1997**, *119*, 10587 and references therein.

(13) Peptoid folding: (a) Armand, P.; Kirshenbaum, K.; Goldsmith, R. A.; Farr-Jones, S.; Barron, A. E.; Truong, K. T.; Dill, K. A.; Mierke, D. F.; Cohen, F. E.; Zuckermann, R. N.; Bradley, E. K. *Proc. Natl. Acad. Sci. U.S.A.* **1998**, *95*, 4309. (b) Kirshenbaum, K.; Barron, A. E.; Goldsmith, R. A.; Armand, P.; Bradley, E. K.; Truong, K. T.; Dill, K. A.; Cohen, F. E.; Zuckermann, R. N. *Proc. Natl. Acad. Sci. U.S.A.* **1998**, *95*, 4303.

(14) *m*-Phenylacetylene oligomer folding: (a) Nelson, J. C.; Saven, J. G.; Moore, J. S.; Wolynes, P. G. *Science* **1997**, *277*, 1793. (b) Prince, R. B.; Okada, T.; Moore, J. S. *Angew. Chem., Int. Ed.* **1999**, *38*, 233. (c) Gin, M. S.; Yokozawa, T.; Prince, R. B.; Moore, J. S. *J. Am. Chem. Soc.* **1999**, *121*, 2643.

(15) α-Aminooxy acid oligomer folding: Yang, D.; Qu, J.; Li, B.; Ng, F.; Wang, X.; Cheung, K.; Wang, D.; Wu, Y. *J. Am. Chem. Soc.* **1999**, *121*, 589 and references therein.

(16) Guanidine oligomer folding: Tanatani, A.; Yamaguchi, K.; Azumaya, I.; Fukutomi, R.; Shudo, K.; Kagechika, H. *J. Am. Chem. Soc.* **1998**, *120*, 6433 and references therein.

(17) Oligopyrrolinone conformations: Smith, A. B.; Guzman, M. C.; Sprengler, P. A.; Keenan, T. P.; Holcomb, R. C.; Wood, J. L.; Carroll, P. J.; Hirschmann, R. *J. Am. Chem. Soc.* **1994**, *116*, 9947.

(18) Pyridine/pyrimidine oligomer folding: (a) Bassani, D. M.; Lehn, J.-M.; Baum, G.; Fenske, D. *Angew. Chem., Int. Ed. Engl.* **1997**, *36*, 1845. (b) Bassani, D. M.; Lehn, J.-M. *Bull. Soc. Chim. Fr.* **1997**, *134*, 897.

10.1021/ja991185g CCC: $18.00
Published on Web 08/06/1999

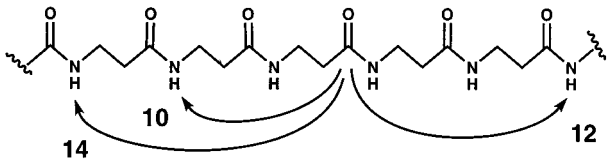

Figure 1. Hydrogen bonds associated with helical β-peptide conformations discussed in the text.

natively, foldamers with well-defined tertiary structures might lead to creation of enzyme-like catalysts. There are several examples of foldamers that adopt discrete secondary structures,[1−18] but no unnatural tertiary structure has yet been reported.

β-Amino acid oligomers ("β-peptides") are among the most thoroughly studied foldamers at present.[1−4] Reports from Seebach et al.[2] and from our laboratory[3] have shown that careful choice of β-amino acid residues and β-peptide sequence can produce several different helices. We have identified β-amino acid residues with high propensities for sheet or reverse turn secondary structure,[3c,d] thus demonstrating that each of the three classes of regular secondary structure observed in proteins can be reproduced in β-peptides. These β-peptides offer greater opportunities to control the secondary structural propensities of individual residues than do conventional peptides (composed of α-amino acids), because the residues we have used have two sp^3 carbons between the carboxyl and amino groups. Bonds between sp^3-hybridized carbon atoms tend to have more clearly defined torsional preferences than do bonds between an sp^3-hybridized carbon and an sp^2-hybridized atom.[20] Further, the two sp^3 atoms of each β-amino acid residue can be incorporated into a ring, thereby reducing residue flexibility, without destroying backbone hydrogen-bonding sites.[3] In contrast, incorporating rings into the α-amino acid backbone will eliminate hydrogen bond donor sites (e.g., proline).

The work of Seebach et al. provides an excellent illustration of residue-based control of β-peptide conformation.[2] These workers have shown that β-peptides containing residues bearing a single β-substituent (all with identical configuration) adopt a helix defined by a series of 14-membered ring hydrogen bonds between backbone amide groups (Figure 1).[2a−c] We refer to this secondary structure as "14-helix", and Seebach et al. designate it "3_1-helix". (For comparison, the familiar α-helix is defined by a series of 13-membered ring hydrogen bonds between backbone amides.) The 14-helix also results if all residues bear a single α-substituent (again, with identical configuation). However, certain "mixed" sequences of α- and β-monosubstituted residues induce formation of a very different helix, defined by alternating 10- and 12-membered ring hydrogen bonds.[2d] β,β-Disubstituted residues disrupt 14-helix formation.[2c]

Our work provides additional examples of residue-based control of β-peptide secondary structure. We have shown that β-amino acid residues bearing one α-substituent and one β-substituent, with appropriate relative stereochemistry, have a high propensity to adopt sheet secondary structure in which the $C_\alpha-C_\beta$ bond of each residue is anti and all carbonyls are oriented in roughly the same direction.[3c,d] In contrast, β-substituted residues or unsubstituted residues (β-alanine) have a much lower propensity to adopt this sheet conformation.[3c] A heterochiral dinipecotic acid segment forms a reverse turn secondary structure.[3d]

We have shown that different β-peptide helical conformations can be induced by use of cycloalkyl restraints. The *trans*-2-aminocyclohexanecarboxylic acid (*trans*-ACHC) residue leads to 14-helix formation,[3a,e,f,21] while, as reported in a preliminary account,[3b] the *trans*-2-aminocyclopentanecarboxylic acid (*trans*-ACPC) residue leads to 12-helix formation. The hydrogen bonds that define these two helices (Figure 1) are oriented in opposite directions relative to the backbone; in contrast, the hydrogen bonds that define the two helices observed in proteins (α-helix and 3_{10}-helix) are oriented in the same direction. Here we describe the synthesis and structural characterization (crystallography and circular dichroism (CD)) of *trans*-ACPC β-peptides. The solid-state structures suggest strategies for design of helical bundle tertiary structures.

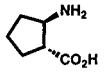

***(R,R)-trans*-ACPC**

Results and Discussion

Synthesis. All β-peptides were prepared from *(R,R)-trans*-ACPC. Synthesis of the optically pure, doubly protected monomer, *tert*-butyloxycarbonyl-*trans*-ACPC ethyl ester (Boc-*trans*-ACPC-OEt), has been reported.[22] This route begins with ethyl *(1R,2S)*-2-hydroxycyclopentanecarboxylate, which we generated via the reported baker's yeast reduction of racemic ethyl 2-oxocyclopentanecarboxylate.[22a] The hydroxyl group is stereospecifically converted to an amino group via Mitsunobu reaction with HN_3, followed by reduction.[22b] We were unable to purify the intermediate azide from the alkene byproduct of the Mitsunobu reaction, so reduction was carried out with the mixture, followed by Boc protection of the amino group. Boc-ACPC-OEt was then purified by chromatography. After deprotection, amide bond formation between Boc-ACPC-OH and H_2N-ACPC-OEt was accomplished using (*N*,*N*-dimethylamino)-propyl-3-ethylcarbodiimide (as the hydrochloride salt (EDCI·HCl)) and 4-(*N*,*N*-dimethylamino)pyridine (DMAP), in DMF solution, to yield Boc-ACPC-ACPC-OEt. At this point, the ethyl ester was replaced by a benzyl ester, and the synthesis of longer β-peptides was accomplished by coupling dimer or longer fragments as described above. The benzyl esters were more crystalline than analogous ethyl esters.

Circular Dichroism. Far-UV circular dichroism (CD) data are commonly used to analyze the secondary structure of conventional peptides.[23] In this spectral region, CD signals arise largely from the amide groups in the peptide backbone. Regular secondary structures (helices, sheets, reverse turns) give rise to characteristic far-UV CD signatures.

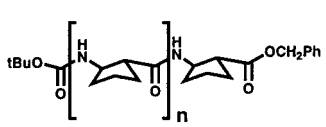

1, n = 0
2, n = 1
3, n = 2
4, n = 3
5, n = 5
6, n = 7

Figure 2 shows far-UV CD data for a homologous series of *trans*-ACPC β-peptides in methanol solution, including dimer **2**, trimer **3**, tetramer **4**, and hexamer **5** (**6** was insufficiently soluble in methanol to be analyzed). The data in Figure 2 have

(19) Fairlie, D. P.; West, M. L.; Wong, A. K. *Curr. Med. Chem.* **1998**, *5*, 29.

(20) (a) Page, M. I.; Jencks, W. P. *Proc. Natl. Acad. Sci. U.S.A.* **1971**, *68*, 1678. (b) Mammen, M.; Shakhnovich, E. I.; Whitesides, G. M. *J. Org. Chem.* **1998**, *63*, 3168.

(21) Independent prediction of 14-helix formation by *trans*-ACHC oligomers: Bode, K. A.; Applequist, J. *Macromolecules* **1997**, *30*, 2144.

(22) (a) Herradón, B.; Seebach, D. *Helv. Chim. Acta* **1989**, *72*, 690−714. (b) Tilley, J. W.; Danho, W.; Shiuey, S.; Kulesha, I.; Swistok, J.; Makofske, R.; Michalewsky, J.; Triscari, J.; Nelson, D.; Weatherford, S.; Madison, V.; Fry, D.; Cook, C. *J. Med. Chem.* **1992**, *35*, 3774.

(23) Woody, R. W. *Circular Dichroism: Principles and Applications*; VCH Publishers: New York, 1994; pp 24−38, 473−496.

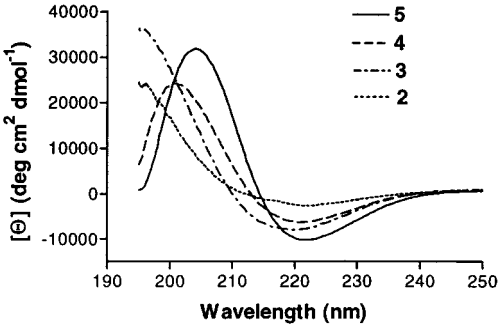

Figure 2. Circular dichroism data in CH_3OH; the molar ellipticity [Θ] values for dimer **2**, trimer **3**, tetramer **4**, and hexamer **5** have been normalized for oligomer concentration and the number of backbone amide groups (one, two, three, and five, respectively).

been normalized for both β-peptide concentration and the number of amide chromophores in each molecule, as is common for conventional peptide CD data. Thus, the vertical axis represents molar ellipticity per residue.

The CD signatures vary significantly across the series **2**−**5**. Since there is no isodichroic point, it is likely that at least three conformational states contribute to these CD spectra. Dimer **2** shows little ellipticity between 215 and 250 nm; below 215 nm, the ellipticity becomes positive. Similar behavior is seen for trimer **3**, except that there is a shallow minimum at ca. 218 nm, and the rise at lower wavelengths is sharper. Tetramer **4** displays a shallow minimum at ca. 220 nm and a maximum at ca. 202 nm. Hexamer **5** has a pattern similar to that of **4**, except that both the minimum and maximum are slightly red-shifted (222 and 207 nm) and more intense for **5** relative to those for **4**. The pattern observed for **5** has been shown to agree with theoretical predictions for the 12-helix CD spectrum.[24] The 12-helical CD signature observed for **5** is quite distinct from the CD signatures of 14-helical β-peptides reported by us[3e,f] and by Seebach et al.[2a−c]

The data for **2**−**5** suggest that the 12-helical conformation becomes more highly populated, i.e., more stable, with additional *trans*-ACPC residues. This trend suggests cooperativity in 12-helix formation, which parallels the well-established cooperativity in α-helix formation by conventional peptides.[25] The 12-helical conformation becomes increasingly stable relative to other conformations as the *trans*-ACPC oligomer grows longer, presumably because the favorable energy of adding residues to the 12-helix out-weighs the energetic cost of helix initiation.

Solid-State Structures. Crystal structures were obtained of both hexamer **5** and octamer **6**. In each crystal, there is only one molecule in the asymmetric unit. Both oligomers display 12-helical conformations in the solid state (Figure 3), with the maximum number of 12-membered ring hydrogen bonds in each case (four for **5** and six for **6**). One molecule of methanol per β-peptide was included in the crystal of **5**. Both methanol and water were included in the crystal of **6**.

The molecules of hexamer **5** are all parallel to one another in the crystal (i.e., the helix axes are parallel, and all molecules display the same orientation of N- and C-termini). This β-peptide is organized into intermolecularly hydrogen-bonded columns in the solid state (Figure 4a). The included methanol molecule participates in this hydrogen-bonding pattern.

Lateral interactions between β-peptide helices are of interest with regard to creating β-peptide tertiary structure. Figure 5

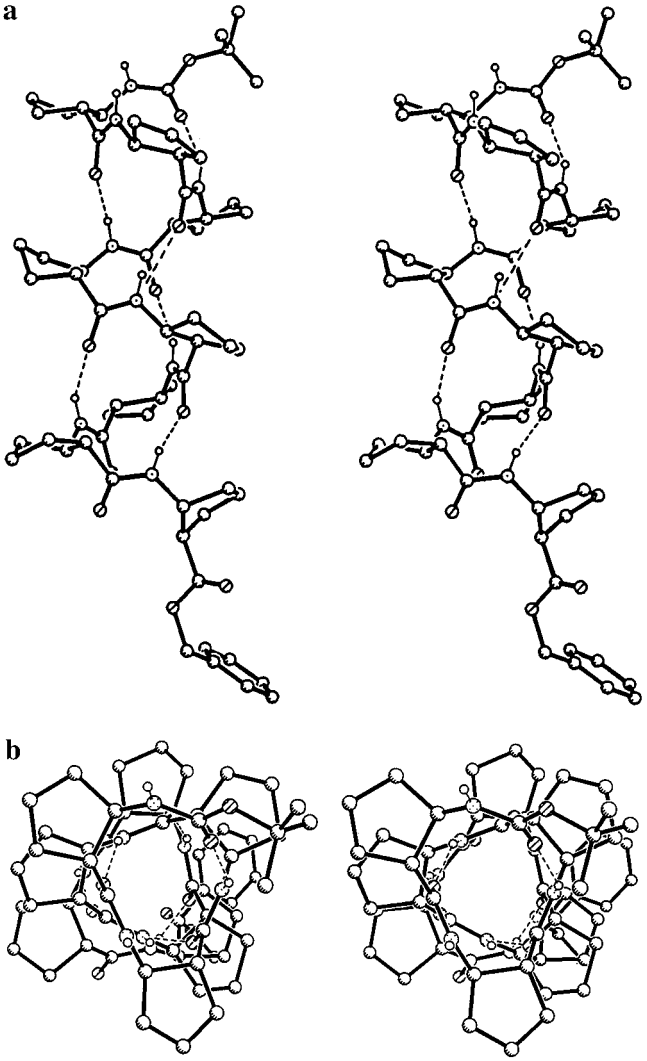

Figure 3. Solid-state structures (stereoviews) of *trans*-ACPC octamer **6** from two perspectives: (a) perpendicular to the helix axis and (b) along the helix axis. Hydrogen atoms other than those attached to nitrogen have been omitted for clarity. Dotted lines indicate hydrogen bonds. Hexamer **5** displays a similar conformation; stereoviews for **5** may be found in the Supporting Information.

illustrates the two types of side-to-side interactions in the crystal of **5**. Interface 1 involves relatively little contact between cyclopentane rings (Figure 6); much of the contact involves the terminal *tert*-butyl and phenyl groups interacting with cyclopentane rings. Interface 2 has extensive intermolecular contact between cyclopentyl rings (Figure 7). Particularly intriguing is the way in which the cyclopentyl ring of residue 3 on one molecule interdigitates between the cyclopentyl rings of residues 2 and 4 on the neighbor (Figure 7a). Each hexamer engages in this type of tight interaction with two neighboring molecules, on opposite sides, which results in infinite strips of tightly packed helices in the crystal.

A spacing-filling view of interface 2, perpendicular to the 12-helix axis (Figure 7b), highlights the extensive and intimate contact between the cyclopentyl rings on neighboring β-peptides. This pairing causes burial of 371 Å^2 of molecular surface from solvent exposure, as estimated using the program MacroModel 6.0 and a probe radius of 1.4 Å (approximating a water molecule; an isolated molecule of **5** in the solid-state conformation displays a solvent-accessible surface area of 1090 Å^2).[26] Such extensive burial of predominantly nonpolar surface could

(24) Applequist, J.; Bode, K.; Appella, D. H.; Christianson, L. A.; Gellman, S. H. *J. Am. Chem. Soc.* **1998**, *120*, 4891.

(25) Hong, Q.; Schellman, J. A. *J. Phys. Chem.* **1992**, *96*, 3987.

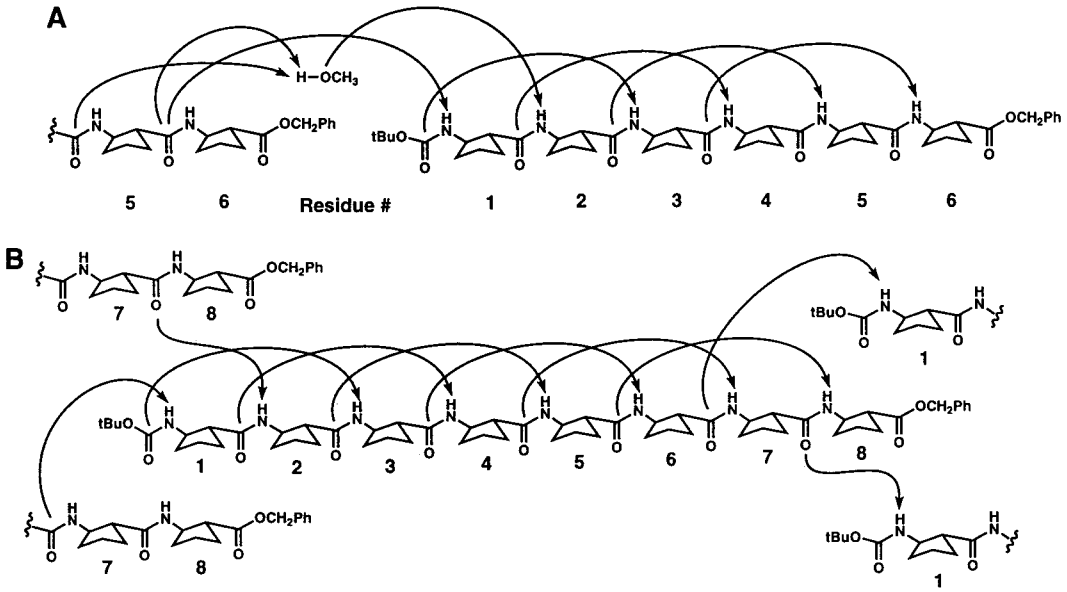

Figure 4. Schematic view of the intra- and intermolecular hydrogen-bonding patterns in *trans*-ACPC oligomer crystals. (a) Hexamer **5**, showing the involvement of a methanol molecule in hydrogen bonds at the helix termini. (b) Octamer **6**, showing that the termini of each molecule form hydrogen bonds to four other molecules.

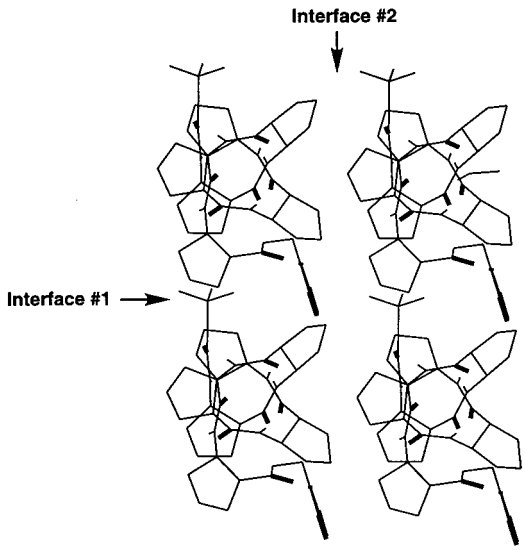

Figure 5. Solid-state packing pattern of hexamer **5**, viewed along the 12-helical axes. Lines indicate bonds between non-hydrogen atoms. See text for detailed discussion.

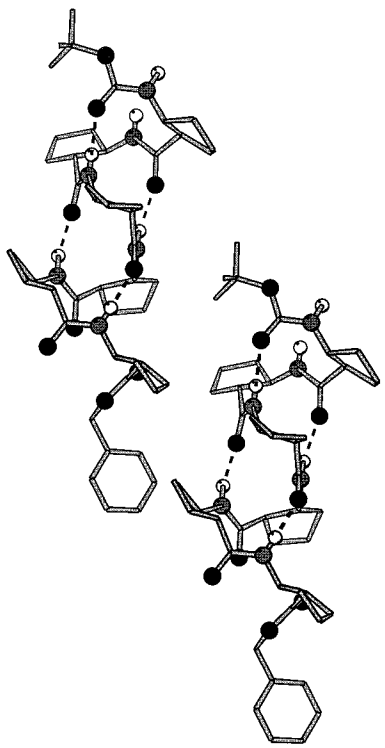

Figure 6. Ball-and-stick view of the lateral interaction between adjacent molecules of hexamer **5** in the solid state (interface 1 in Figure 5).

provide a significant hydrophobic driving force for helix−helix interaction in aqueous solution. If the helices were part of a single β-peptide, then the helix−helix interaction would constitute tertiary structure formation.

In the crystal of octamer **6**, there are both parallel and antiparallel neighbor relationships (i.e., all helix axes are parallel, but neighbors display both identical and opposite orientations of N- and C-termini), in contrast to the exclusively parallel packing of hexamer **5**. Intermolecular hydrogen bonding in **6** occurs only between β-peptide molecules with parallel orientation. The end-to-end intermolecular hydrogen-bonding pattern for octamer **6** is illustrated in Figure 4b. The solvent molecules included in the crystal of **6** do not appear to hydrogen bond to the β-peptide.

The packing pattern of octamer **6** is more complex than the packing pattern of hexamer **5**. Figure 8 provides a schematic representation of the octamer packing pattern viewed along the 12-helix axis. Individual octamer molecules are represented by squares with N- and C-termini labeled. Disordered solvent molecules (water and methanol) lie along one side of each octamer; the solvent molecules and the C-terminal benzyl groups occupy the apparent gaps in Figure 8.

In the crystalline form of octamer **6** there are two types of side-to-side interactions between β-peptide helices that involve extensive contact between cyclopentyl rings. The tighter of these two lateral interactions occurs between antiparallel neighbors

(26) Mohamdi, F.; Richards, N. G. J.; Guida, W. C.; Liskamp, R.; Lipton, M.; Caufield, C.; Chang, G.; Hendrickson, T.; Still, W. C. *J. Comput. Chem.* **1990**, *11*, 440.

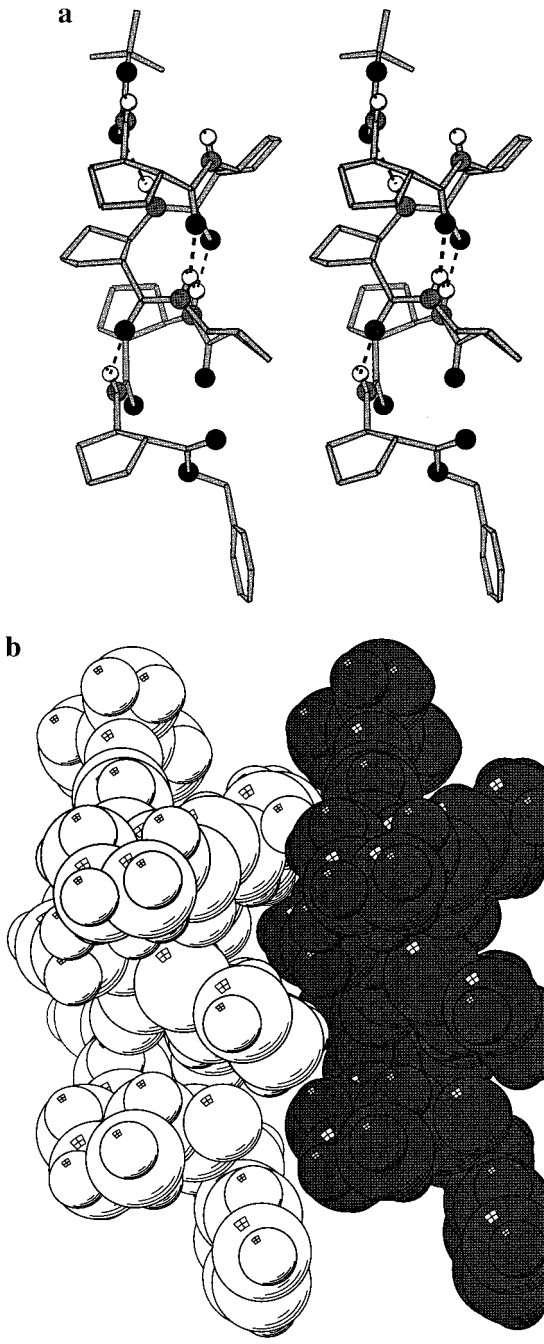

Figure 7. Lateral interactions between adjacent molecules of hexamer **5** in the solid state (interface 2 in Figure 5). (a) Ball-and-stick view, perpendicular to the 12-helix axis. (b) Space-filling view, perpendicular to the 12-helix axis (same perspective as in panel a). These and other space-filling views were generated with the program Molscript.[31] (These are not stereoviews.)

(interface 1 in Figure 8). This interaction is illustrated in detail in Figure 9. The interface is comprised largely of the cyclopentyl rings of residues 3, 5, and 8 and the *tert*-butyl group of the N-terminal Boc group. This antiparallel pairing causes burial of 652 Å^2 of molecular surface from solvent exposure (1.4 Å probe radius; an isolated molecule of **6** in the solid-state conformation displays a solvent-accessible surface area of 1330 Å^2).

The looser of the two types of side-to-side interactions between β-peptide helices in crystalline **6** occurs between parallel neighbors (interface 2 in Figure 8). This interaction is illustrated in detail in Figure 10. Each octamer forms this type of interface with two neighboring molecules, on opposite sides.

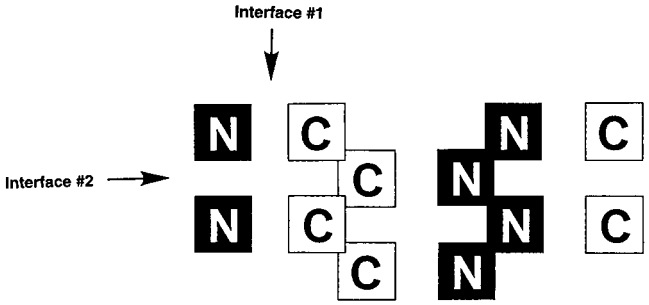

Figure 8. Solid-state packing pattern of octamer **6** viewed along the 12-helix axis, which corresponds approximately to the crystallographic *b* axis. N and C represent the amino and carboxyl termini of the β-peptide molecules. See text for detailed discussion.

The interface is defined by residues 1, 3, and 6 on one molecule and residues 2, 5, and 7 on the other. This lateral interaction is analogous to but looser than the parallel lateral interaction between hexamers in crystalline **5** (Figure 7), although the relative orientations of the helices are not identical. This parallel pairing of molecules of **6** causes burial of 325 Å^2 (1.4 Å probe radius).

Conclusions. The crystallographic and CD data presented here show that short β-peptides comprised of (*R*,*R*)-*trans*-ACPC residues adopt a well-defined helical secondary structure. This helix, involving a series of interlocking 12-membered ring hydrogen bonds between backbone amide groups, is distinct from other secondary structures that have been observed for short β-peptides. Seebach et al.[2a−c] and we[3a,e,f,21] have previously reported different types of β-peptide oligomers that adopt a 14-helical conformation. Poly[α-isobutyl-L-aspartate] and related β-peptide homopolymers have been proposed to adopt the 14-helix; interestingly, 16-, 18-, and 20-helical conformations, but not the 12-helix, have also been proposed for these polymers.[27]

A major long-range goal of our β-peptide studies is to create protein-like tertiary structures. The solid-state packing patterns observed for hexamer **5** and octamer **6** suggest that it will be possible to achieve this goal with *trans*-ACPC-based β-peptides. The helical bundle is one of the simplest tertiary packing motifs in proteins: α-helical segments pack side-to-side, with short loops connecting the helices.[28] The helix surfaces that contact one another are typically dominated by nonpolar residues, and burial of the hydrophobic surface provides a driving force for tertiary folding in aqueous solution. Relatively short conventional peptides designed to adopt amphiphilic α-helical conformations (i.e., α-helices that display discrete hydrophobic and hydrophilic surfaces) have been shown to self-assemble into helical bundles in solution and in the solid state.[29] Incorporation of several amphiphilic α-helical segments into a longer polypeptide allows de novo creation of protein tertiary structures.[30] This

(27) (a) Fernández-Santin, J. M.; Aymamí, J.; Rodríguez-Galán, A.; Muñoz-Guerra, S.; Subirana, J. A. *Nature* **1984**, *311*, 53. (b) Fernández-Santin, J. M.; Muñoz-Guerra, S.; Rodríguez-Galán, A.; Aymamí, J.; Lloveras, J.; Subirana, J. A.; Giralt, E.; Ptak, M. *Macromolecules* **1987**, *20*, 62. (c) Bella, J.; Alemán, C.; Fernández-Santin, J. M.; Alegre, C.; Subirana, J. A. *Macromolecules* **1992**, *25*, 5225. (d) López-Carrasquero, F.; Alemán, C.; Muñoz-Guerra, S. *Biopolymers* **1995**, *36*, 263.

(28) Cohen, C.; Parry, D. A. D. *Proteins: Struct., Funct. Genet.* **1990**, *7*, 1.

(29) (a) Regan, L.; DeGrado, W. F. *Science* **1988**, *241*, 976. (b) Mutter, M.; Vuilleumier, S. *Angew. Chem., Int. Ed. Engl.* **1989**, *28*, 535. (c) Bryson, J. W.; Betz, S. F.; Lu, H. S.; Suich, D. J.; Zhou, H. X.; O'Neil, K. T.; DeGrado, W. F. *Science* **1995**, *270*, 935. (d) Walsh, S. T. R.; Cheng, H.; Bryson, J. W.; Roder, H.; DeGrado, W. F. *Proc. Natl. Acad. Sci. U.S.A.* **1999**, *96*, 5486.

(30) Sheldrick, G. M. *SHELXTL Version 5 Reference Manual*; Bruker-AXS: 6300 Enterprise Dr., Madison, WI 53719-1173, 1994.

(31) Kraulis, P. J. *J. Appl. Crystallogr.* **1991**, *24*, 946.

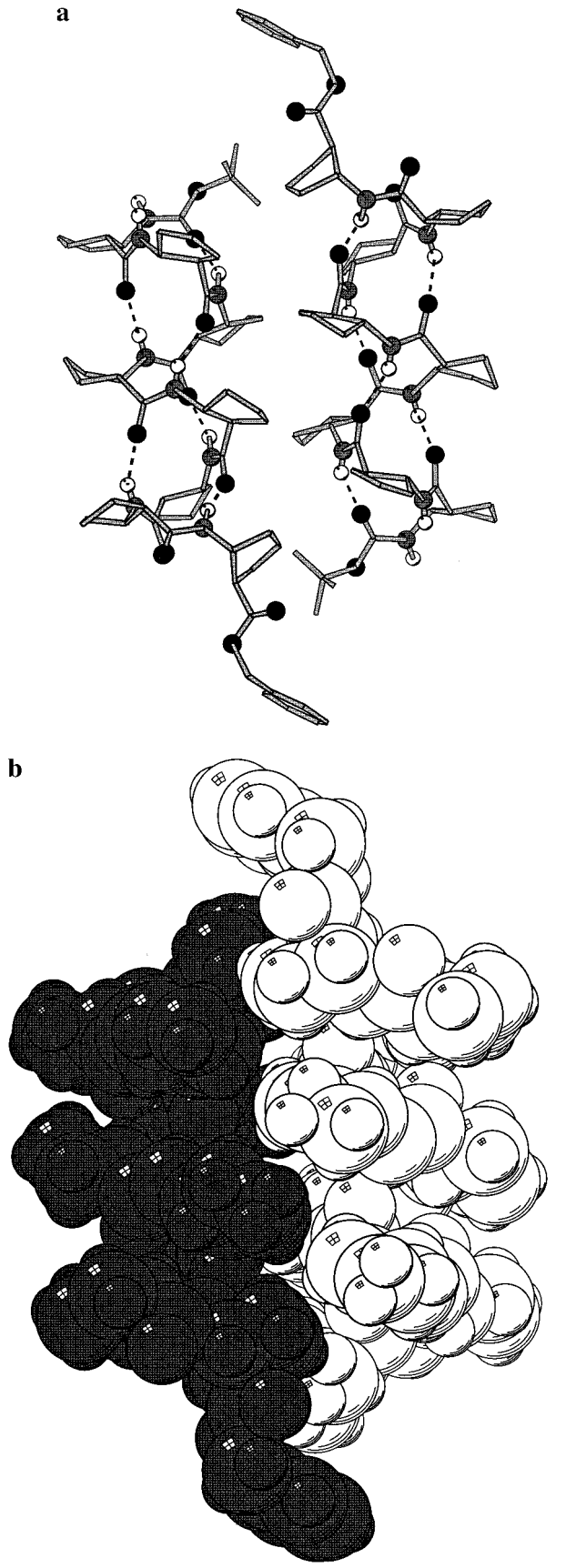

Figure 9. Close packing between antiparallel pairs of octamer **6** in the solid state (interface 1 in Figure 8). (a) Ball-and-stick view, perpendicular to the 12-helix axis. (b) Space-filling view, perpendicular to the 12-helix axis (same perspective as in panel a).

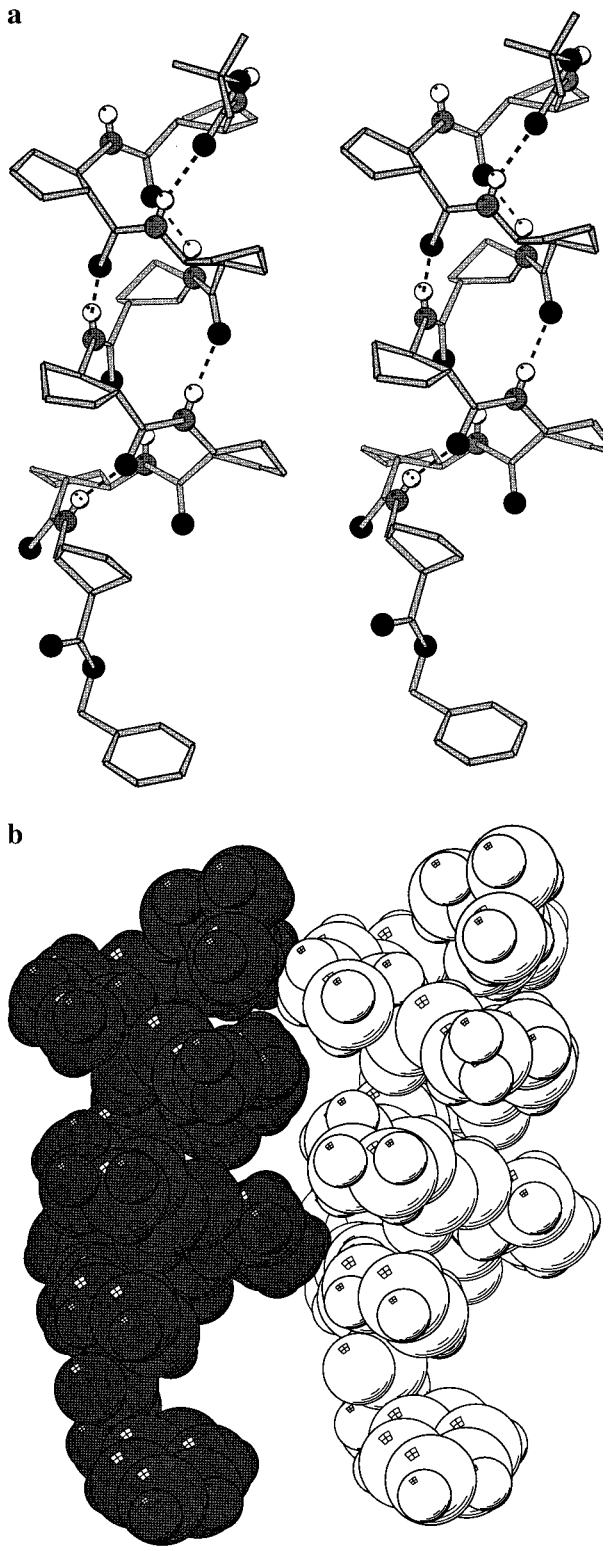

Figure 10. Close packing between parallel pairs of octamer **6** in the solid state (interface 2 in Figure 8). (a) Ball-and-stick view, perpendicular to the 12-helix axis. (b) Space-filling view, perpendicular to the 12-helix axis (same perspective as in panel a). (These are not stereoviews.)

strategy should be transferable to β-peptides if we can prepare polar analogues of *trans*-ACPC. The lateral packing patterns observed in the crystals of **5** and **6** suggest that properly spaced *trans*-ACPC residues can be used to create complementary hydrophobic surfaces on 12-helical β-peptides; we are currently testing this hypothesis.

Experimental Section

General Procedures. Melting points (mp) were obtained on a Thomas-Hoover capillary melting point apparatus and are uncorrected. Infrared spectra (IR) were obtained on a Mattson Polaris FT-IR spectrophotometer or a Nicolet 740 FT-IR spectrometer. Absorption maxima are reported in wavenumbers (cm^{-1}) and are standardized to the 1601 cm^{-1} reference peak of polystyrene. Proton nuclear magnetic resonance (^1H NMR) spectra were recorded in deuterated solvents on a Bruker AC-300 (300 MHz) or Bruker AMX (500 MHz) spectrometer. Chemical shifts are reported in parts per million (ppm, δ) relative to tetramethylsilane (δ 0.00). If tetramethylsilane was not present in the deuterated solvent, the residual protio solvent is referenced. ^1H NMR splitting patterns are designated as singlet (s), doublet (d), triplet (t), or quartet (q). All first-order splitting patterns are assigned on the basis of the appearance of the multiplet. Splitting patterns that could not be interpreted or easily visualized are designated as multiplet (m) or broad (br). Coupling constants are reported in hertz (Hz). Carbon nuclear magnetic resonance (^{13}C NMR) spectra were recorded on a Bruker AC-300 spectrometer. Chemical shifts are reported in ppm (δ) relative to the central line of the $CDCl_3$ triplet (δ 77.0) or the CD_3OD septet (δ 49.0). Carbon resonances were assigned using distortionless enhancement by polarization transfer (DEPT) spectra obtained with a phase angle of 135°: (C) not observed; (CH) positive; (CH_2) negative; (CH_3) positive. Mass spectra (MS) were obtained using a Kratos MS-80 mass spectrometer with a magnetic sector and direct probe when electron impact (EI, 70 eV) was the ionization method. Fast-atom bombardment (FAB) mass spectra were obtained on a Micromass AutoSpec (Cs ion gun) with magnetic sector and direct probe using 3-nitrobenzyl alcohol as the ionization matrix. DMF was distilled from ninhydrin under vacuum at 25 °C and stored over activated 3-Å molecular sieves, under N_2, at 4 °C. Unless otherwise noted, all other commercially available reagents and solvents were purchased from Aldrich and used without further purification, except for 4 N HCl in dioxane, which was purchased from Pierce. Analytical thin-layer chromatography (TLC) was carried out on Whatman TLC plates precoated with silica gel 60 (250 μm layer thickness). Visualization was accomplished using either a UV lamp, potassium permanganate stain (2 g of $KMnO_4$, 13.3 g of K_2CO_3, 3.3 mL of 5% (w/w) NaOH, 200 mL of H_2O), or ninhydrin stain (0.5 g of ninhydrin, 150 mL of *n*-butanol, 5 mL of glacial acetic acid). Column chromatography was performed on EM Science silica gel 60 (230−400 mesh). Solvent mixtures used for TLC and column chromatography are reported in v/v ratios.

Boc-*trans*-ACPC-OEt was prepared by a procedure similar to that of Tilley and co-workers.[22b] (*CAUTION: HN_3 is very toxic and a volatile gas!*) NaN_3 (4 g, 0.06 mol) was suspended in water (4 mL) and benzene (25 mL). This solution was cooled to 10 °C in an ice bath, and concentrated H_2SO_4 (3.5 mL) was added dropwise to the solution in a fume hood while the temperature was maintained at 10 °C. After addition was complete, the solution was stirred an additional 15 min, and the layers were then separated. The organic layer was dried over Na_2SO_4 to yield a solution of HN_3 in benzene. The concentration of acid in the benzene solution was determined by taking 1 mL of the solution, diluting with water (10 mL), adding 1 drop of phenolphthalein indicator, and titrating with 0.14 N NaOH. An HN_3 concentration of 1.0−1.7 M was typically obtained. Unused HN_3 solution was immediately destroyed by addition of excess NaOH. Ethyl (1*R*,2*S*)-2-hydroxycyclopentanecarboxylate[22a] (2.2 g, 14 mmol) was dissolved in dry benzene (60 mL), and triphenylphosphine (5.5 g, 21 mmol) was added, followed by HN_3 solution (13 mL, 1.61 M, 21 mmol). Diethyl azodicarboxylate (2.7 mL, 17 mmol) was dissolved in dry benzene (10 mL), and the solution was added dropwise over 1 h to the solution of alcohol, triphenylphosphine, and HN_3 so that the reaction temperature did not go above room temperature. During the addition, white solid formed. After addition was complete, the mixture was stirred an additional 8 h. The solvent was removed on a rotary evaporator, and the products were purified by SiO_2 column chromatography, eluting with CH_2Cl_2, to afford 1.3 g of yellow liquid that was a mixture of ethyl (1*R*,2*R*)-azidocyclopentanecarboxylate and ethyl 1-cyclopentenecarboxylate. This mixture was dissolved in THF (15 mL), and water (0.3 mL) was added, followed by triphenylphosphine (3.67 g, 14 mmol). The solution was stirred 18 h. Di-*tert*-butyl dicarbonate (3.1 g, 14 mmol) was then added, and the resulting solution was stirred 48 h. The solvent was removed on a rotary evaporator, and the product was purified by SiO_2 column chromatography, eluting with 5:1 hexane/ethyl acetate, to afford 0.66 g (18% yield) of Boc-*trans*-ACPC-OEt as a white solid. Crystals were obtained by vapor diffusion of *n*-heptane into a solution of Boc-*trans*-ACPC-OEt in 1,2-dichloroethane: mp 74 °C; $[\alpha]^{D}_{23} = -47.1$ (*c* 0.68, $CHCl_3$); IR (KBr) 3342 (N−H), 3045−2703 (broad), 1717 (C═O), 1700, 1526, 1364, 1309, 1251, 1160, 1029, 863, 801 cm^{-1}; ^1H NMR ($CDCl_3$, 300 MHz) δ 4.56 (br, 1H, NH), 4.18−4.09 (m, 3H, CH_3CH_2 and *t*-BuOCONHC*H*), 2.56 (q, J = 7 Hz, 1H, EtOOCC*H*), 2.18−1.63 (m, 4H), 1.53−1.38 (m, 11H), 1.43 (s, CH_3), 1.26 (t, J = 7 Hz, 3H, CH_3CH_2); ^{13}C NMR ($CDCl_3$, 75.4 MHz) δ 174.7 (C), 155.2 (C), 79.2 (C), 60.5 (CH2), 56.0 (CH), 50.9 (CH), 33.0 (CH_2), 28.3 (CH_3), 22.8 (CH_2), 14.1 (CH_3).

Boc-(*trans*-ACPC)$_2$-OEt. (*R*,*R*)-Boc-*trans*-ACPC-OEt (0.35 g, 1.4 mmol) was dissolved in methanol (20 mL) and water (7 mL). LiOH·H_2O (0.57 g, 13.6 mmol) was added. The resulting solution was cooled to 0 °C, and H_2O_2 (0.75 mL of a 30.8% aqueous H_2O_2 solution, 6.8 mmol) was added. The reaction was placed in a cold room at 5 °C and stirred 20 h. While the reaction was still cold, aqueous Na_2SO_3 (2.7 g in 12 mL of water, 21.4 mmol) was added. The solution was moved out of the cold room, and the methanol was removed on a rotary evaporator. The resulting solution was adjusted to pH 2 with 3 N HCl, and the aqueous solution was then extracted with CH_2Cl_2 (3×, 75 mL total). The organic extracts were dried over Na_2SO_4, concentrated, and put under vacuum to yield 0.21 g (67% yield) of white solid (Boc-*trans*-ACPC-OH). Boc-*trans*-ACPC-OEt (0.23 g, 0.9 mmol) was dissolved in 4 N HCl/dioxane (2 mL). The solution was stirred for 1 h, and then the solvent was removed under a stream of N_2 and the residue further dried under vacuum to give H_2N-*trans*-ACPC-OEt. Boc-*trans*-ACPC-OH was dissolved in DMF (3 mL) and transferred via cannula to the flask containing H_2N-*trans*-ACPC-OEt. DMAP (0.13 g, 1.1 mmol) was added, followed by EDCI·HCl (0.38 g, 1.98 mmol). The reaction was stirred for 36 h under N_2. The solvent was removed under a stream of N_2, and the residue was further dried under vacuum. To this residue was added 1 N HCl (a few milliliters). The resulting white solid was collected by suction filtration and dried under vacuum to afford 0.3 g (91% yield) of Boc-(*trans*-ACPC)$_2$-OEt. Fluffy crystals were obtained by vapor diffusion of *n*-heptane into a solution of Boc-(*trans*-ACPC)$_2$-OEt in 1,2-dichloroethane: mp 180−181 °C dec; IR (KBr) 3279 (N−H), 2963, 2872, 2771, 1734 (C═O), 1692, 1653, 1558, 1365, 1311, 1181, 1152, 1022, 678 cm^{-1}; ^1H NMR ($CDCl_3$, 300 MHz) δ 7.72 (br, 1H, NH), 4.66 (br, 1H, NH), 4.41 (quintet, J = 7 Hz, 1H, CONHC*H*), 4.13 (*ABX*$_3$, J_{AX} = 7 Hz, J_{AB} = 11 Hz, 1H, CH_3CH_2), 4.12 (*ABX*$_3$, J_{BX} = 7 Hz, J_{AB} = 11 Hz, 1H, CH_3CH_2), 3.95 (quintet, J = 7 Hz, 1H, CONHC*H*), 2.68 (dt, J = 8, 7 Hz, 1H, NHCOC*H*), 2.58 (m, 1H, NHCOC*H*), 2.15−1.34 (m, 21H), 1.45 (s, CH_3), 1.24 (t, J = 7 Hz, 3H, CH_3CH_2); ^{13}C NMR ($CDCl_3$, 75.4 MHz) δ 174.9 (C), 173.0 (C), 156.4 (C), 80.0 (C), 60.4 (CH_2), 56.3 (CH), 54.6 (CH), 53.2 (CH), 50.7 (CH), 33.5 (CH_2), 32.7 (CH_2), 28.4 (CH_3), 27.4 (CH_2), 24.1 (CH_2), 23.1 (CH_2), 14.2 (CH_3); EI-MS m/z (M^+) calcd for $C_{19}H_{32}N_2O_5$ 368.2311, obsd 368.2296; FAB-MS m/z 369.3 ($M + H^+$), 313.2 ($M^+ - t$-Bu), 267.2 (M^+ − Boc).

Boc-(*trans*-ACPC)$_2$-OBn (2). Boc-(*trans*-ACPC)$_2$-OEt (0.26 g, 0.7 mmol) was dissolved in methanol (10 mL) and water (4 mL). LiOH·H_2O (0.3 g, 7 mmol) was added, the resulting solution was cooled to 0 °C, and H_2O_2 (0.35 mL of a 30.8% aqueous H_2O_2 solution, 3.5 mmol) was added. The reaction was placed in a cold room at 5 °C and stirred 23 h. While the reaction was still cold, aqueous Na_2SO_3 (1.6 g in 12 mL of water, 13 mmol) was added. The solution was moved out of the cold room, and the methanol was removed on a rotary evaporator. The resulting solution was adjusted to pH 2 with 3 N HCl, and the aqueous solution was then extracted with CH_2Cl_2 (3×, 100 mL total). The combined organic extracts were dried over Na_2SO_4, concentrated, and dried under vacuum to yield 0.2 g (81% yield) of white solid Boc-(*trans*-ACPC)$_2$-OH. This acid was dissolved in DMF (3 mL), and Cs_2CO_3 (0.2 g, 0.7 mmol) was added, followed by benzyl bromide (0.09 mL, 0.8 mmol). The resulting solution was stirred under N_2 for 18 h, and then the solvent was removed under a stream of N_2. The residue was dissolved in 15 mL of water and extracted with $CHCl_3$ (3×, 40

mL total). The organic extracts were dried over $MgSO_4$, concentrated, and dried under vacuum. The product was purified by SiO_2 column chromatography, eluting with 20:1 $CHCl_3$/acetone to give 0.21 g (85% yield) of Boc-(*trans*-ACPC)$_2$-OBn as a white solid. Fluffy crystals were obtained by vapor diffusion of *n*-heptane into a solution of Boc-(*trans*-ACPC)$_2$-OBn in 1,2-dichloroethane: mp 142 °C dec; ^{1}H NMR ($CDCl_3$, 300 MHz) δ 7.79 (br, 1H, NH), 7.38−7.28 (m, 4H, ArH), 5.16 (*A*B quartet, J = 12 Hz, 1H, ArCH_2), 5.08 (A*B* quartet, J = 12 Hz, 1H, ArCH_2), 4.59 (br, 1H, NH), 4.44 (quintet, J = 7 Hz, 1H, CONHC*H*), 3.85 (quintet, J = 7 Hz, 1H, CONHC*H*), 2.75 (q, J = 7 Hz, 1H, NHCOC*H*), 2.56 (m, 1H, NHCOC*H*), 2.16−1.26 (m, 21H), 1.44 (s, CH_3); FAB-MS *m*/*z* 453.4 (M^+).

Boc-(*trans*-ACPC)$_3$-OBn (3), **Boc-(*trans*-ACPC)$_4$-OBn (4)**, **Boc-(*trans*-ACPC)$_6$-OBn (5), and Boc-(*trans*-ACPC)$_8$-OBn (6)** were prepared by coupling smaller fragments, using procedures analgous to those described for the synthesis of dimer **2**. Characterization data for these oligomers may be found in the Supporting Information.

Crystallography. The X-ray diffraction data were measured using a Bruker SMART CCD area detector on a four-circle *P*4 diffractometer equipped with Mo *K*α radiation (λ = 0.710 73 Å). Data for both compounds were collected as a series of ϕ scan frames, each with a width of 0.3°/frame. The exposure times were 30 s/frame for **5** and 60 s/frame for **6**. Empirical absorption corrections for both compounds were based on equivalent measured intensities. Both structures were solved by direct methods and refined by full-matrix least-squares, minimizing ΔF^2 (ref 30). For both compounds, the non-hydrogen atoms were refined with anisotropic displacement parameters. The positions for hydrogen atoms were calculated from model geometry. For compound **6**, disorder was observed in two of the five-membered rings (via ring flips), the phenyl end of the peptide, and the two methanol sites. Restraints for the positional and displacement parameters of the disordered atoms were required in order to achieve convergence.

Circular Dichroism. Dry peptide samples were weighed on a Cahn microanalytical balance and dissolved in an appropriate amount of HPLC grade methanol. Sample cells of 1- and 5-mm path length were used. Data were collected on a Jasco J-715 spectrometer at 20 °C. Baseline spectra were recorded with only solvent in the cell. Baseline spectra were subtracted from the raw data. Data were converted to ellipticity (deg cm^2 dmol^{-1}) according to the following equation:

$$[\Theta] = \psi M_r/100lc$$

where ψ is the CD signal in degrees, M_r is the molecular weight divided by the number of chromophores, l is the path length in decimeters, and c is the concentration in grams per milliliter.

Acknowledgment. This research was supported by the NIH (GM-56414). D.H.A. was supported in part by a Chemistry−Biology Training Grant from NIGMS and by a fellowship from Procter & Gamble. The X-ray instrument and computers used in this study were provided by funds from NSF (CHE-9310428) and the University of Wisconsin.

Supporting Information Available: Tables of crystal data, structure solution and refinement, atomic coordinates, bond lengths and angles, torsion angles, and hydrogen bond parameters for **5** and **6** (PDF). This material is available free of charge via the Internet at http://pubs.acs.org.

JA991185G